EEET ECOLOGICAL ENGINEERING & ENVIRONMENTAL TECHNOLOGY

Ecological Engineering & Environmental Technology, 2026, 27(3), 223–238
https://doi.org/10.12912/27197050/218210
ISSN 2719–7050, License CC-BY 4.0

Received: 2026.01.21
Accepted: 2026.02.20
Published: 2026.03.01

Mapping ground collapse vulnerability in a climate-responsive karst area: A GIS and AHP approach in Abda Doukkala, Morocco

Mustapha Rharouss[1*], Latifa Ouadif[1], Mariame Bouchaqour[2], Fatiha Aitelhaj[1], Ilyass Dhimine[1]

[1] Laboratory of Applied Geophysics, Geotechnics, Engineering Geology and Environment, Mohammadia Engineering School, Mohammed V University, Rabat, Morocco
[2] Euromed Polytechnic School, Euromed University of Fes, Fez 30030, Morocco
* Corresponding author's e-mail: m.rharouss@research.emi.ac.ma

ABSTRACT

The Doukkala-Abda region, situated in central-western Morocco, known for its karst cavities and collapses. These underground collapses pose a major risk, particularly to the population. Hence, the purpose of this article, which aims to build susceptibility maps of karst collapses in the community of Moul El Bergui belonging to this region. This susceptibility map was created based on Geographic Information system method and analytical hierarchy process. Several factors are responsible for karst collapse. Nine parameters were chosen in the present study. These factors are slope, altitude, aspect, hydrographic density, fracture density, land cover, normalized difference vegetation index, precipitation and lithology. Their maps were prepared with ArcGIS software. Subsequently, AHP was employed to rank and weight factors according to their importance in causing karst collapses. Finally, the combination of index maps in ArcGIS allowed the creation of the final vulnerability map, which is divided into five classes, from very low to very high. The results illustrate high prevalence of moderate and high classes. Based on identified collapses and geophysical prospection in the area, the resulting map was validated using Area Under the Curve. AUC value obtained of 92.6% reflects an excellent degree of prediction. Thus, these findings can help decision makers in land use planning to prevent areas of potential collapses within such environments.

Keywords: environmental sustainability, geographic information system, analytical hierarchy process, geophysics, Abda-Doukkala, collapse mapping.

INTRODUCTION

The phenomenon of karst collapse presents a major hazard to population, infrastructures such as roads (Xie et al., 2022), and buildings (Zhou et al., 2024), but can also affect agricultural fields. The Abda Doukkala region is marked by a complex karst environment, which leads to landslides. These later are documented in numerous geological and geophysical articles, as discussed recently by Boualla et al. (2016, 2021), Bouzerda et al. (2020) and Rharouss et al. (2025). With industrial, urban and agricultural development in this region, the ground surface collapses has motivated decision-makers to assess associated hazards and to delineate areas most susceptible to doline formation. This study was interested in the area known as Moul El Bergui.

To assess this susceptibility, and to explain and predict the occurrence of this natural phenomenon, several methods can be applied. These methods are used according to the variability of the techniques and tools available. They can be divided into two groups: qualitative or quantitative (Yalcin et al., 2011). Qualitative methods are subjective, based on expert judgment, in which experts determine susceptibility levels according to their perception (Wang and Li, 2017). Quantitative methods, on the other hand, use automatic calculations to provide an objective and reproducible assessment, as discussed by Erener et al. (2016). Sometimes, qualitative assessment

requires a thorough understanding of the factors involved in ground movements. Environmental factors are classified, prioritized, and weighted according to their presumed importance, using for example the analytical hierarchy process. This method can be considered as semi quantitative (Zighmi et al., 2025).

The assessment of karst collapse passes through sequential steps. Firstly, landslides inventory, followed by selection and preparation of input factors. Then, determination of their relative weights and finally validation of results. Susceptibility maps illustrate potential collapses based on analysis of parameters that caused them in the past, as illustrated by Guzzetti et al. (2025). It assumes that future landslides are likely to occur under similar conditions.

Accordingly, this study aims to develop a GIS-based ground-collapse susceptibility map using the analytical hierarchy process (AHP), providing a quantitative tool to identify areas at high risk and support effective land-use planning and hazard mitigation.

MATERIALS AND METHODS

The methodology for producing a karst collapse susceptibility map begins with the collection of data on key triggering factors, including lithology, slope, land use, and hydrological conditions, from multiple sources such as geological surveys, remote sensing data, and field measurements. Each factor is represented as an index map in ArcGIS. The analytical hierarchy process is then applied to assign relative weights to these factors based on their influence on collapse susceptibility (Wei et al., 2021). Weighted index maps are combined using a weighted sum model to generate the final susceptibility map. The resulting map is validated through comparison with a comprehensive inventory of observed collapse events and spatial correlation with geophysical survey data (ERT and radar). Model performance is quantitatively assessed using the receiver operating characteristic (ROC) curve and the area under the curve (AUC), ensuring that areas identified as high-risk correspond to actual collapse occurrences. Figure 1 presents a schematic workflow of the methodology.

Study area

The current study focused on Moul El Bergui area located near to Safi province, part of Marrakech Safi region in central-western Morocco (Fig. 2). It is a predominantly rural municipality within the Doukkala Abda region, covering an area of approximately 166.06km².

Data acquisition and collection

This step aims to gather, organize, and prepare all the data needed to develop the thematic maps used in the analysis. This data corresponds to parameters that are decisive in the production of the collapse susceptibility map, since they

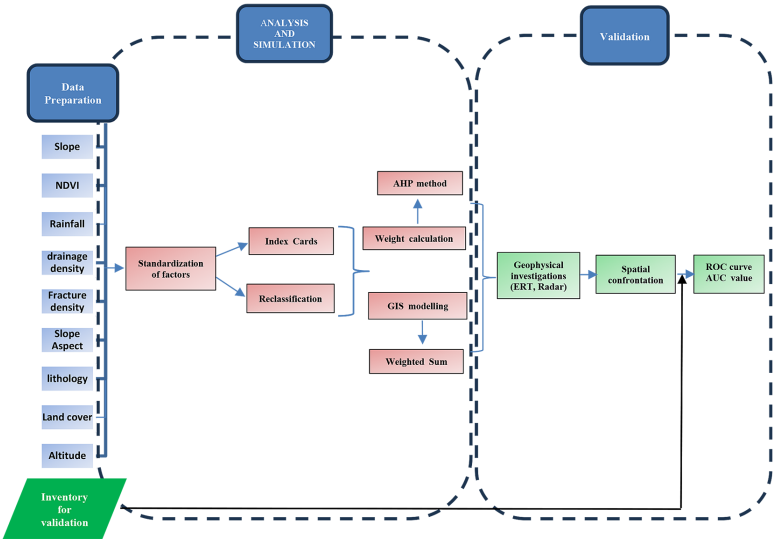

Figure 1. Flowchart of the adopted methodology

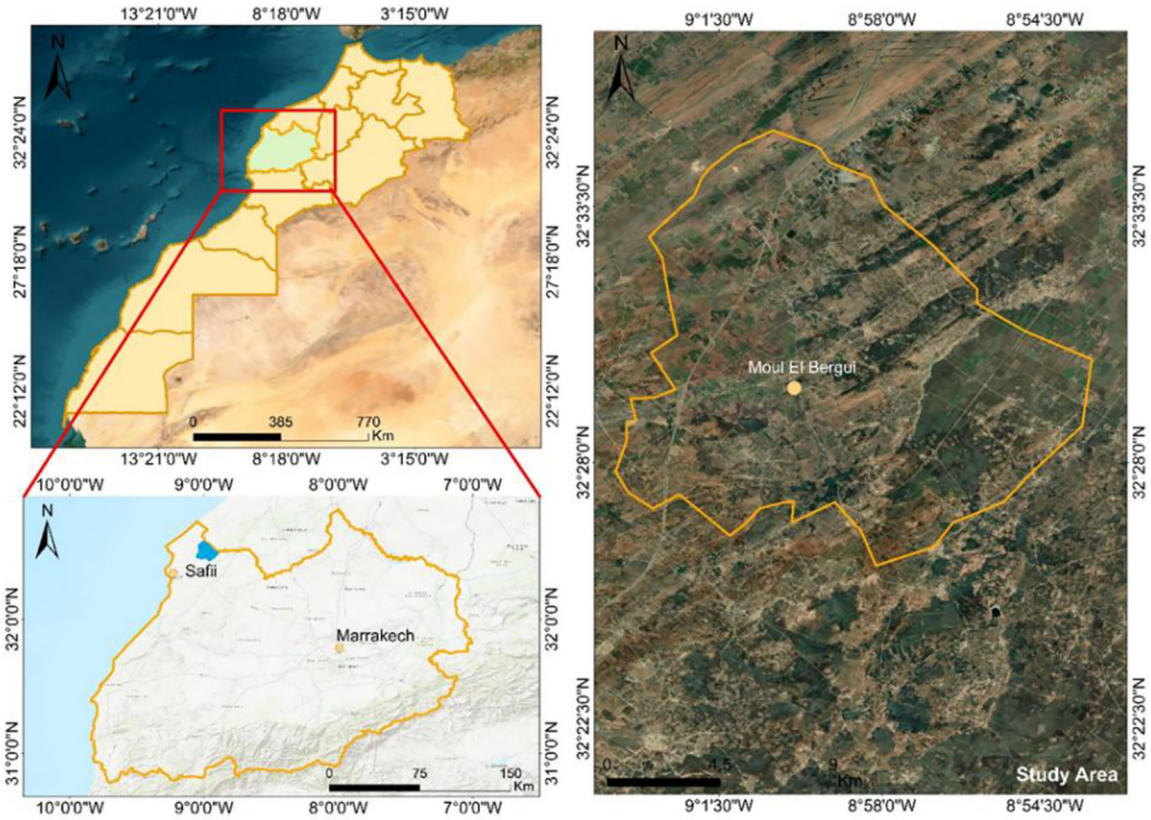

Figure 2. Location of the study area

directly influence the accuracy and reliability of the results obtained from the spatial analysis.

The parameters used in this study include slope, elevation, hydrographic density, fracture density, land cover, normalized difference vegetation index, aspect, precipitation and lithology. Table 1 presents all these parameters, their respective data sources, and their scales of analysis.

Creation of a digitized map illustrating lithology of area required the use of the geological map of the Meseta, covering the region between Mechra Ben Abbou and Safi (Abda-Doukkala and the Rehamna massif).

NDVI is determined from information on quantity and density of vegetation by considering the near infrared and visible red bands of the electromagnetic spectrum (Ait El haj et al., 2023). It is expressed by Equation 1:

$$NDVI = \frac{\rho NIR - \rho RED}{\rho NIR + \rho RED} \quad (1)$$

where: ρNIR represents the reflectance in the near infrared, ρRED represents the reflectance in the red band.

Processing of collected data and creation of index cards

The index maps were created using GIS method (ArcGIS software). For each parameter, a detailed description used to create susceptibility map will be presented later.

Weighting of collapse susceptibility factors and creation of the final susceptibility map

Analytic hierarchy process method was used in the present study, to determine weights of factors triggering landslide susceptibility, which were then integrated into a weighted sum model in a GIS environment.

Presentation of the AHP method

Analytic hierarchy process is a multi-criteria decision-making method that has been described by many authors (Ibraheem et al., 2016; Ben Brahim et al., 2022). It allows criteria and alternatives to be structured and ranked in order to facilitate the decision-making process. This approach emphasizes the importance of hierarchical structuring, pairwise comparisons, and the consideration of preferences.

Table 1. List of selected parameters and data used

Parameter	Data source	Scale / Resolution
Slope, altitude, aspect	Digital Elevation Model (DEM) downloaded from the ASF Data Search platform https://search.asf.alaska.edu/	12.5 m
Hydrographic density	Derived from the ALOS PALSAR DEM (ASF DAAC)	12.5 m
Fracture density, lithology	Geological map downloaded from https://geograchid.blogspot.com/2016/05/telecharger-kml-cartes-geologiques-200.html?m=1	1/200 000
Land use, NDVI	Satellite images (Landsat 8, Sentinel 2) from USGS Earth Explorer https://earthexplorer.usgs.gov/	10 m
Precipitations	Climate data (CHRS data portal) https://chrsdata.eng.uci.edu/	PERSIANN-CCS 0.04° x 0.04°

AHP method process

The AHP is based on the following main steps, as detailed by Bouchaqour et al. (2023):

- Step 1: Define the objective

The aim is to clearly identify the objective of the decision and specify the criteria and associated alternatives (Elhamdouni et al., 2022).

- Step 2: Build the hierarchy

This step involves establishing a hierarchy of criteria and alternatives. The top level of the hierarchy is generally the overall objective, followed by criteria and sub-criteria, and finally alternatives (Ayadi et al., 2010).

- Step 3: Evaluate pairwise comparisons

At this stage, we establish pairwise comparisons between the elements of each level of the hierarchy. A scale of values is used to express preferences: from 1 to 9, where 1 means equal preference and 9 means extremely strong preference (Table 2).

- Step 4: Build a comparison matrix

Based on the peer evaluations, we construct a comparison matrix for each level of the hierarchy. Each matrix is a representation of the relative preferences between the elements.

$$A=[aij]=\begin{pmatrix} 1 & \cdots & aij \\ \vdots & \ddots & \vdots \\ \frac{1}{aij} & \cdots & 1 \end{pmatrix} \quad (2)$$

We assign (aij) to the cell in column "i" and row "j" of the criterion deemed important. Next, we insert the value of "1/aij" in the cell deemed least important in the comparison. The priority vector is then determined by following these steps (Bouroumine et al., 2020):

- add up each column,
- divide each element of the matrix by the sum of its corresponding column,
- calculate average of elements for each line of the matrix.

At this level, we use comparison matrices to calculate relative weights. This allows us to assign numerical values to elements at each level of hierarchy.

- Step 5: Check consistency

This consists of evaluating the consistency of judgments by calculating the consistency ratio for each comparison matrix. If the consistency ratio exceeds a pre-established threshold, it may be necessary to review the judgments or refine the hierarchy.

The consistency ratio is calculated by Equation 3:

$$CR = 100 \times IC/ACI \quad (3)$$

where: *CI* – is the consistency index calculated following Equation 4:

$$IC = \lambda max - \frac{n}{n-1} \quad (4)$$

Table 2. Pairwise comparison scale

Degree of importance	Definition
1	Equal importance of both elements: Equally important
3	Low importance to another element: Slightly more important
5	One element is more important than other: Significantly more important
7	One element is much more important than the other: Much more important
9	One element is absolutely more important than the other: Absolutely more important

where: λmax – maximum eigenvalue, n – number of elements being compared, ACI – is average consistency index (Table 3).

However, if the CR>10%, it is essential to review the pairwise comparison, improving consistency.

Validation of the final susceptibility map

Any mapping and risk assessment study requires the collection of as much information as possible on the location of collapses. Given the study area size (166.06 km²) and collapse frequency, their characterization was based mainly on the visual interpretation of high-resolution satellite images. 22 points of collapses were identified in study area (Fig. 3).

Thus, final map of karst collapse was validated based on identified collapses in the study area, also detected by geophysical studies such as Electrical Resistivity Tomography and Ground Penetrating Radar as discussed by Boualla et al. (2016, 2021).

RESULTS

Creation of index maps using ArcGIS

The hypsometric map

The hypsometric map, also known as an elevation map, shows the altitudinal distribution of the relief. It is created by establishing altitude classes based on the digital elevation model (DEM) used (Pourghasemi et al., 2018).

The method adopted is based on reclassifying elevation values using the "Reclassify" tool in ArcGIS to obtain the desired classes. The result is a hypsometric map in the form of a raster image with five elevation classes: 127–153 m, 153–166 m, 166–177 m, 177–192 m, and 192–216 m (Fig. 4).

The raster map is then converted into a polygon shapefile using the Raster to Polygon tool. Next, the Dissolve tool is applied to merge features of the same classes, calculate areas, and export the resulting attribute table to Excel for statistical analysis of this factor (Table 4).

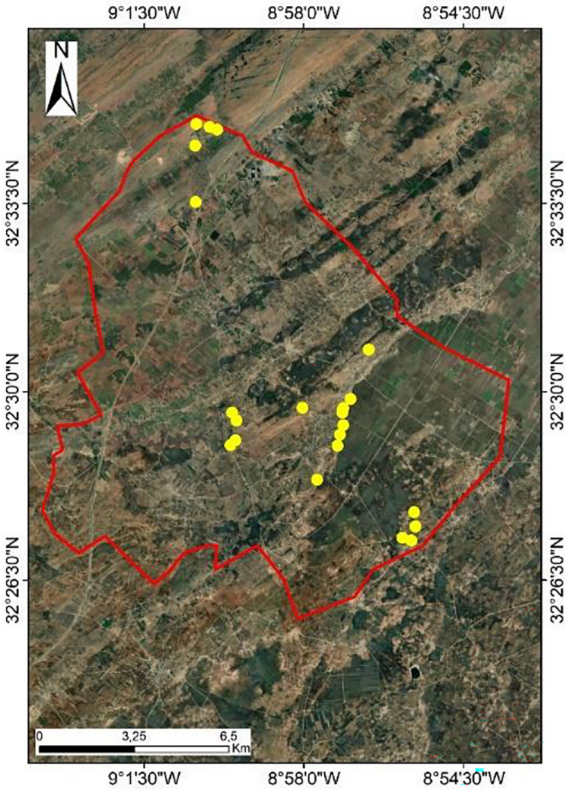

Figure 3. Identified collapses in study area

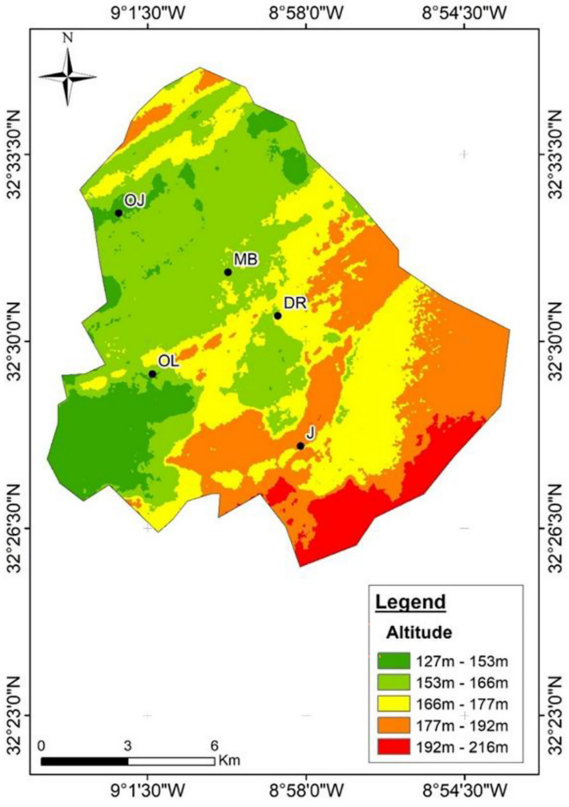

Figure 4. Hypsometry of Moul EL Bergui

Table 3. Average consistency index

Dimension of matrix	1	2	3	4	5	6	7	8	9	10
Average consistency index ACI	0.00	0.00	0.58	0.90	1.12	1.24	1.32	1.41	1.45	1.49

Table 4. Percentage area of elevation classes

Elevation classes	Class area (km²)	Occupied area (%)
127–153 m	17.86	10.75
153–166 m	54.73	32.96
166–177 m	45.41	27.34
177–192 m	38.54	23.21
192–216 m	9.51	5.72

A general analysis of the hypsometric map of Moul el Bergui reveals the main morphological features of the area. This system is represented by the colors yellow, orange, and red (≥ 166 m), which characterize the highest altitudes on the hypsometric map. We note that the most represented altitude classes are those of 153–166 m (32.96%) and 166–177 m (27.35%) as shown in Figure 5.

The slope gradient map

Studying slope gradients is fundamental for understanding slope dynamics. Slope gradients enable us to identify areas with an increased risk of instability. The slope gradient map was created in ArcGIS from digital elevation model using the Slope tool. Values obtained were then grouped using the Reclassify tool into five classes: very low (0–1.3°), low (1.3–3°), medium (3–4.6°), high (4.6–7°) and very high (7–15.6°) as illustrated in Figure 6.

Similarly as before, after analyzing data and obtaining statistical results, the areas occupied by each slope gradient class were expressed as a percentage. Thus, low slope is the most represented class in the study area (51.52%), followed by very low slope (28.86%), medium slope (15.31%), high slope (3.62%) and very high slope (0.69%), the latter being almost non-existent, which reflects the very low presence of areas with very steep slope (Figure 7).

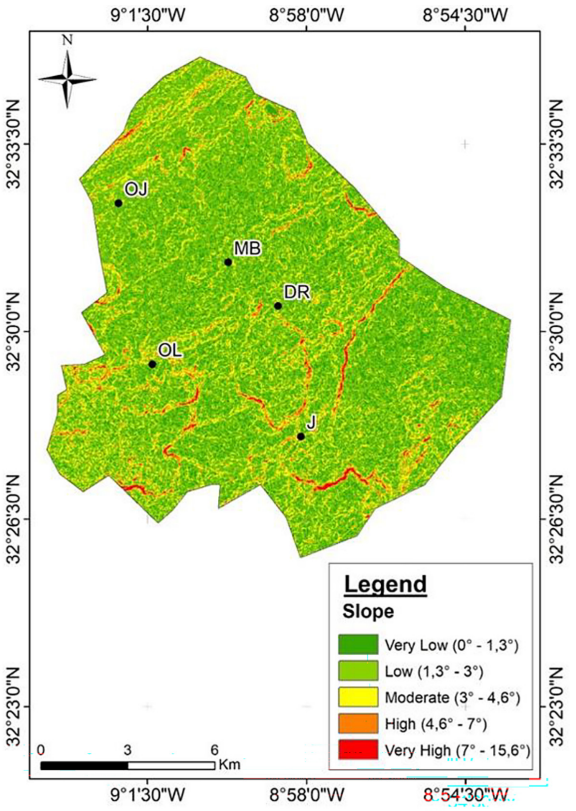

Figure 6. Slope gradient of Moul El Bergui

The NDVI map

The Normalized Difference Vegetation Index is an indicator of vegetation density and health. It is calculated from Landsat 8 satellite images downloaded from United States Geological Survey (Earth Explorer) platform according to Equation 5 below using the raster calculator tool in ArcGIS.

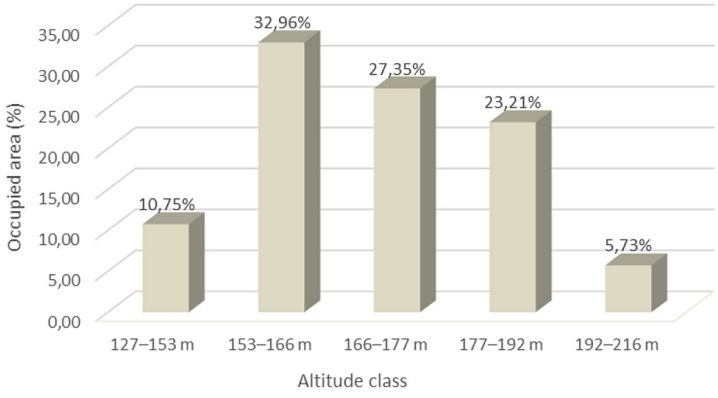

Figure 5. Bar chart of the percentage area of each elevation class

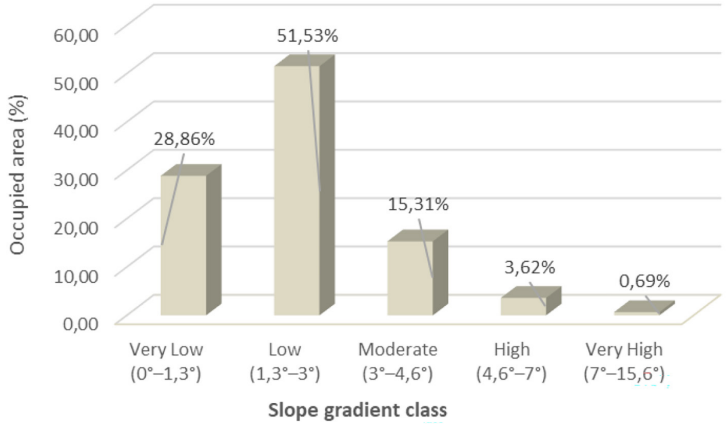

Figure 7. Bar chart of the area occupied by slope gradient class

$$NDVI = \frac{(B5 - B4)}{(B5 + B4)} \quad (5)$$

where: *B5* – represents the near infrared,
B4 – represents the red band.

The values obtained were then grouped using the reclassify tool into five classes: very low (0.07–0.1), low (0.1–0.13), medium (0.13–0.19), high (0.19–0.29) and very high (0.29–0.54) as illustrated in Figure 8.

In the same way, the analysis of statistical results shows that low NDVI is most represented class in the study area (59.34%), followed by the very low (32.05%), medium (6.35%), high (1.53%), and very high (0.72%) NDVI classes as shown in Figure 9.

The hydrographic network density map

The hydrographic network, through its density, provides information on several physical processes, such as the relative share of surface flow, underground flow, and the influence of relief. The density map of the Moul El Bergui hydrographic network was produced with the same methodology as that used for fractures, using the "line density" tool in ArcGIS. This time, the calculation is based on the segmented polyline shapefile of the hydrographic network, generated from the digital elevation model using the Fill, Flow Direction, low Accumulation, Con and Stream Order tools.

The result is a density map of the hydrographic network expressed in km², which was then reclassified using the Reclassify tool into five classes: very low (0–0.8), low (0.8–1.7), medium (1.7–2.6), high (2.6–3.8), and very high (3.8–6.1) as illustrated in Figure 10.

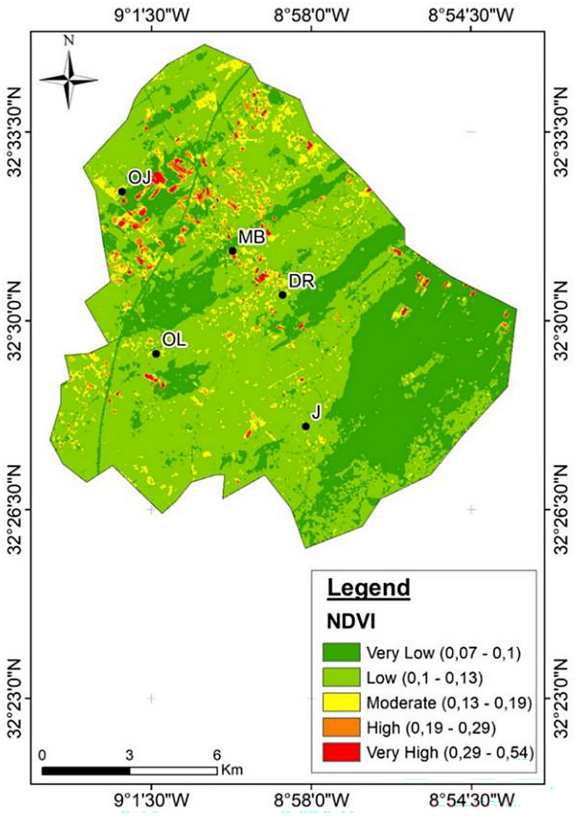

Figure 8. The NDVI map of Moul El Bergui

Following the same detailed procedure described above for the hypsometric factor using ArcGIS software, the resulting attribute table was exported to Excel. The percentage of each class was calculated by dividing the area occupied by that class by the total area of the study region and multiplying the result by 100. The statistical analysis shows that low-density (26.79%) and medium-density (25.56%) areas together account for nearly 50% of the region, followed by high-density (15.74%) and very high-density (7.07%) areas (Figure 11).

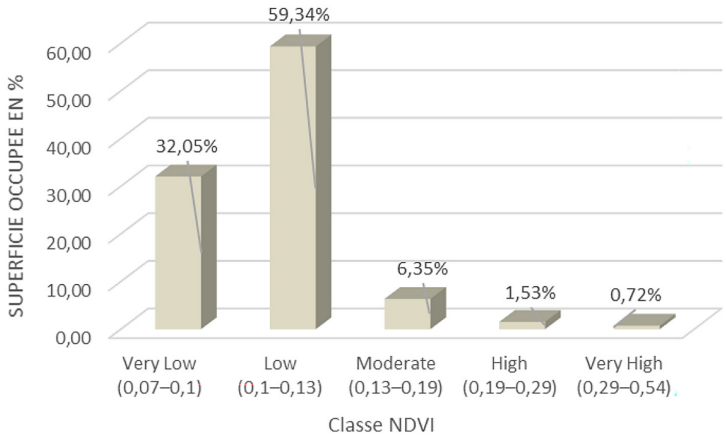

Figure 9. Bar chart of the area occupied by NDVI class

The rainfall map

The rainfall map for Moul El Bergui was created using annual precipitation data for the period 2019–2024, obtained via the CHRS climate data portal. Spatial interpolation was performed in ArcGIS using the IDW (Inverse Distance Weighting) tool. The result is a map of average annual precipitation, which was then reclassified using the Reclassify tool into five classes: very low (168–174.5 mm/year), low (174.5–180.1 mm/year), medium (180.1–185 mm/year), high (185–191.1 mm/year), and very high (191.1–199.9 mm/year) (Figure 12).

Analysis of statistical results, as illustrated in Figure 13, shows that 41.18% of the region's area receives annual precipitation between 180.1 and 185 mm, while 24.62% corresponds to the range 174.5–180.1 mm, 21.08% between 185 and 191.1 mm, 8.10% between 191.1 and 199.9 mm, and 5.02% between 168 and 174.5 mm.

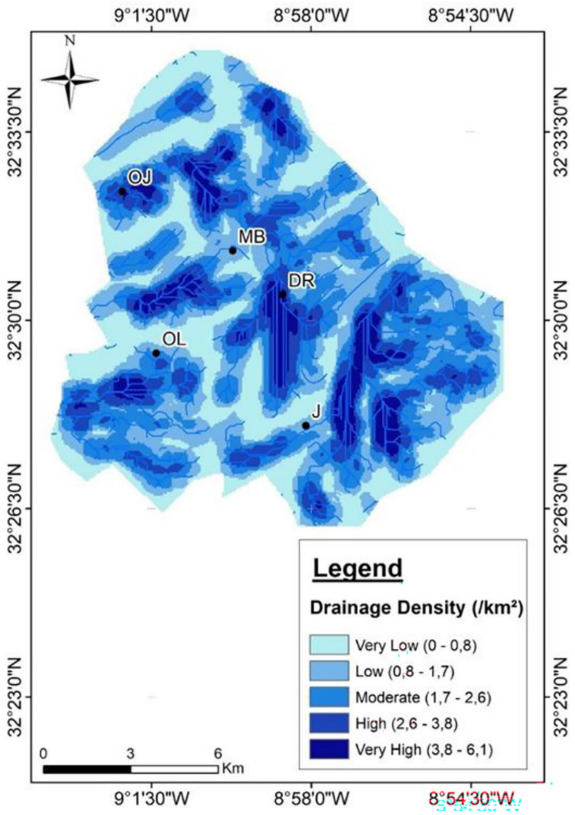

Figure 10. The hydrographic network density map of Moul El Bergu

The slope exposure map

The exposure of a slope represents its orientation relative to north, which helps us understand the influence of orientation on sunlight, humidity, and, more broadly, on geomorphological processes. For several years, geographic information systems (GIS) have offered numerous specialized modules for the automatic generation of exposure maps from digital elevation models (DEM). The exposure map of Moul El Bergui was created in ArcGIS with the Aspect tool, using our DEM.

The result is an exposure map, which was then reclassified using the Reclassify tool into nine classes, according to the angle of orientation of the slopes in a clockwise direction: Flat, North (0–22.5° and 337.5–360°), Northeast (22.5–67.5°), East (67.5–112.5°), Southeast (112.5–157.5°), South (157.5–202.5°), Southwest (202.5–247.5°), West (247.5–292.5°), Northwest (292.5–337.5°)(Fig. 14).

Analysis of the results of areas occupied by each exposure class, as illustrated in Figure 15, shows that north-facing areas are the most extensive (17.5 to 22.93%), followed by

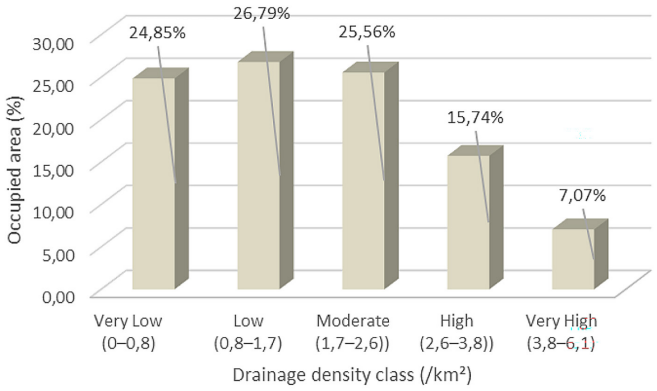

Figure 11. Bar chart of the area occupied by hydrographic network density class

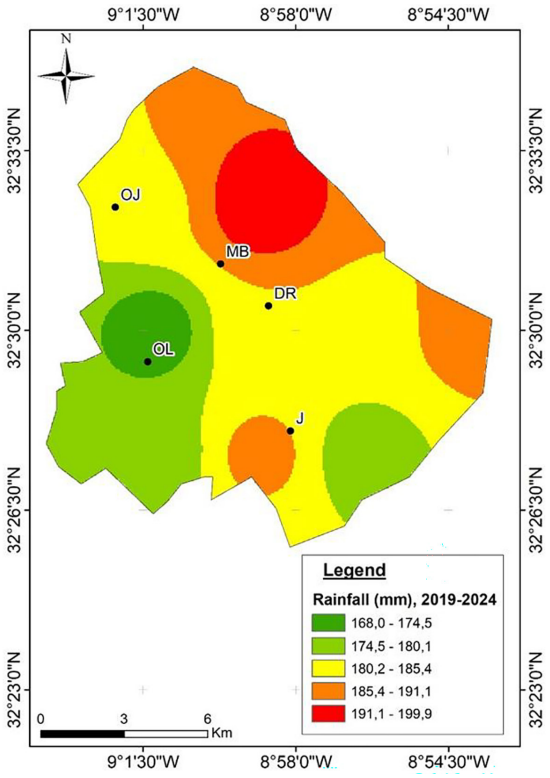

Figure 12. The rainfall map of Moul El Bergui

south-facing areas (11.51%) and northwest-facing areas (10.09%), while the other exposure classes each account for less than 10% of the surface area.

The fracture density map

The fracture density map was created using the Hillshade tool, utilizing the digital elevation model (DEM) to highlight fracture zones. Several lineaments oriented in different directions were digitized in ArcGIS. These lineaments were then segmented into polylines, and the density was calculated per km² using line density tool. Result was reclassified using the reclassify tool into five classes: very low (0–0.28), low (0.28–0.78), medium (0.78–1.31), high (1.31–1.92), and very high (1.92–3.38) as illustrated in Figure 16.

After analysis of the results of areas occupied by each fracture density class (Fig. 17), we note that areas with very low fracture density dominate the study area (44.32%), followed by low (21.09%), medium (19.21%), and high (10.41%) classes.

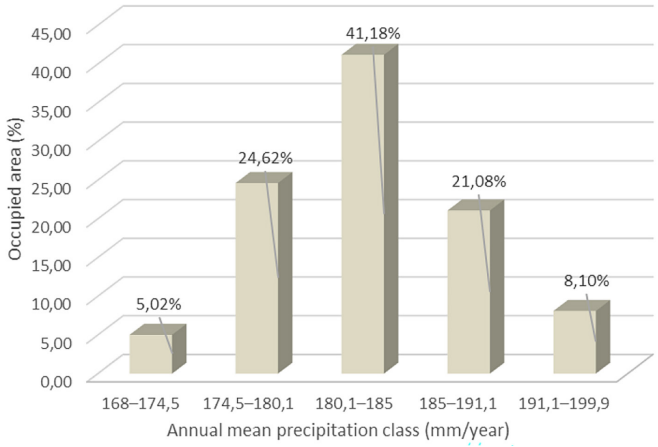

Figure 13. Bar chart of the area occupied by mean annual precipitation class

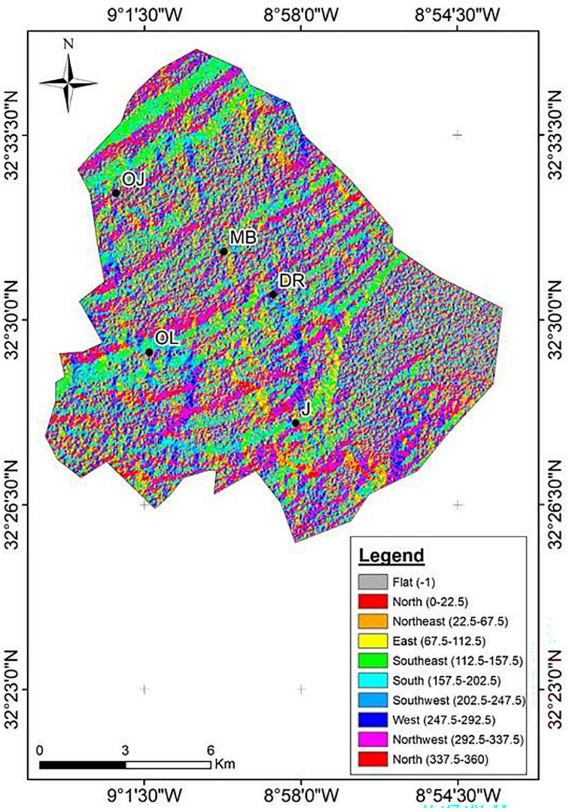

Figure 14. Slope exposure map in Moul El Bergui

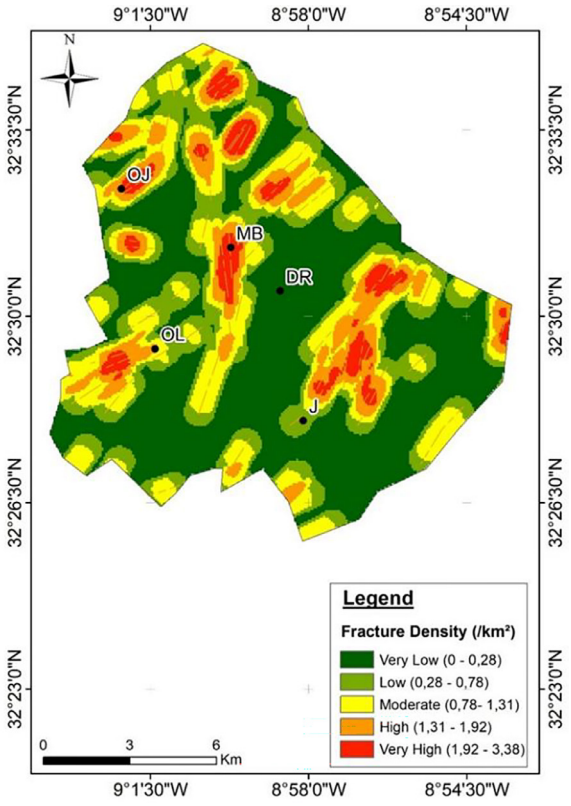

Figure 16. The fracture density map of Moul El Bergui

The facies map

The stability of slopes depends on the geological facies, the nature of the rocks, and the configuration of geological structure.

Facies map was produced in two stages: firstly, the existing geological map was georeferenced, and then the various geological layers were digitized in the form of polygons, based on the map legend. The map obtained is as follows (Figure. 18).

After analysis of the results of areas occupied by each class in the study area (note that these areas refer to outcropping formations), we note that Plio-Quaternary formations (molasse, sandstone, lumachelle) represent 48.63% of the surface area, the Lower Cretaceous (red clay, limestone) 37.13%, modern deposits (silty alluvium) 8.26%, and Quaternary formations (silty soils with gravel) 5.97% (Fig. 19). The presence of a significant percentage of Cretaceous surface area,

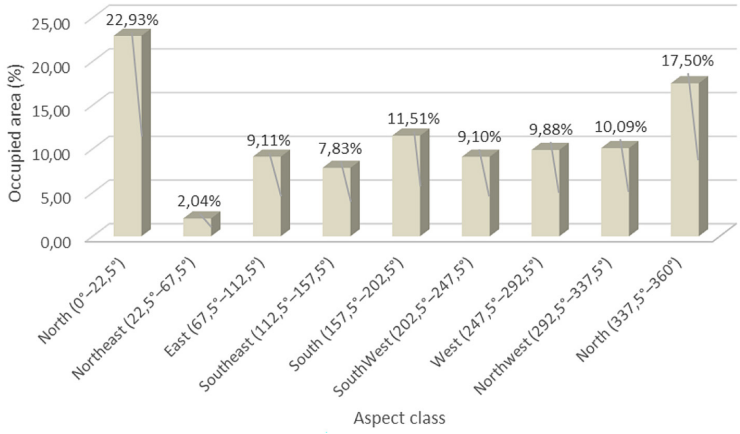

Figure 15. Bar chart of the area occupied by exposure class

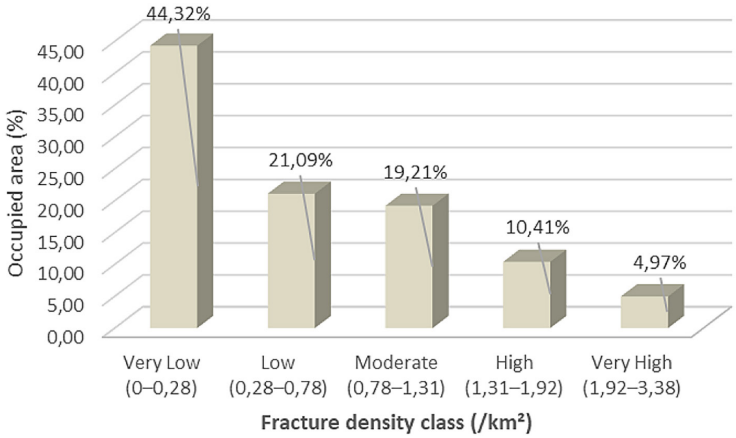

Figure 17. Bar chart of the area occupied by fracture density class

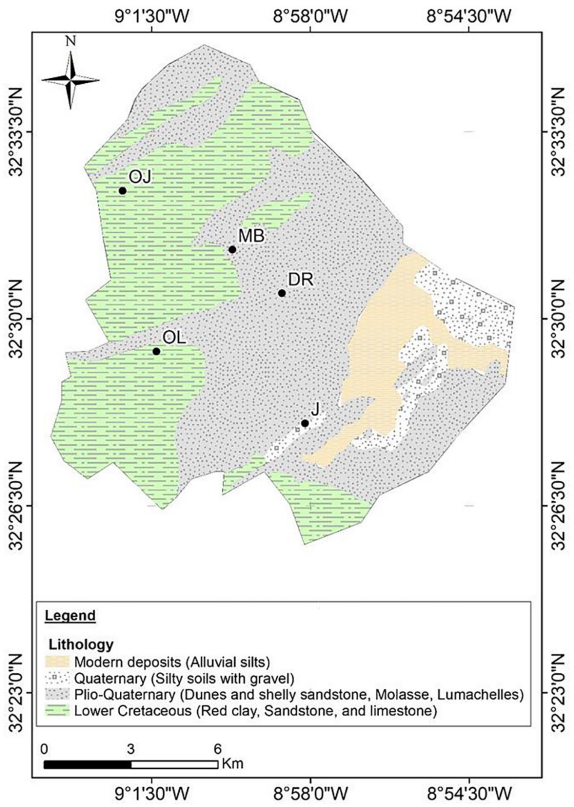

Figure 18. Lithology map of Moul El Bergui

rich in limestone, is particularly significant for the analysis of landslides, as these hard rocks can create steep, rigid slopes, promoting local instability.

The land cover map

Land cover map was reclassified using Reclassify tool representing water, trees, crops, built areas and bare ground, as shown in Figure 20.

Analysis of the results of areas occupied by each class, as illustrated in Figure 21, shows that water and trees (forest) cover a very small percentage of the region, between 0 and 0.02%, and therefore occupy a negligible portion of the region's surface area. The area consists mainly of crops (71.39%) and bare soil (23.39%), while urban areas account for 5.20% of the surface area.

Weightings of factors of susceptibility to collapse

The AHP method described in detail above was applied to our case study. Following the pairwise comparison, the judgment matrix was drawn up as shown in Table 5.

Once the judgment matrix was completed, we weighted it by dividing each element of the matrix by the sum of the corresponding column. The elements of the priority vector are calculated as the average of each row of the weighted matrix (Table 6).

After calculating the priority vector, it is essential to check the consistency of the matrix by calculating its consistency ratio, as detailed in the steps of the hierarchical analysis process (Table 7).

We end up with a CR = 8.37 % <10%, which verifies the consistency of the judgment matrix. As a result, Table 8 shows the weighting of the judgment criteria.

DISCUSSION

Final collapse susceptibility map

The importance of each factor was expressed by the product of the weighted values of the different classes and the weight of the

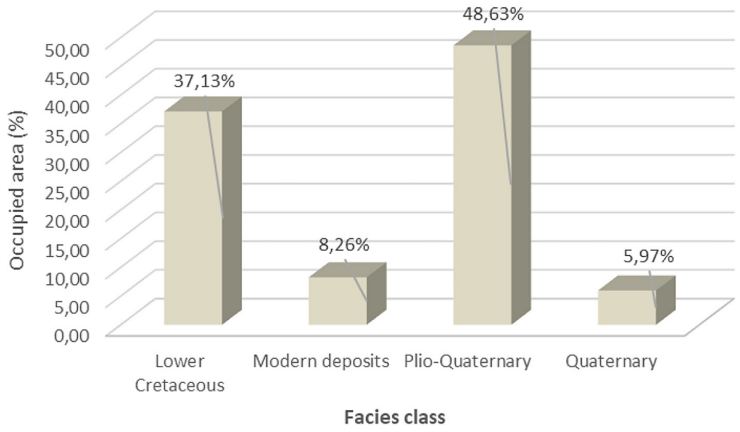

Figure 19. Bar chart of the area occupied by facies class

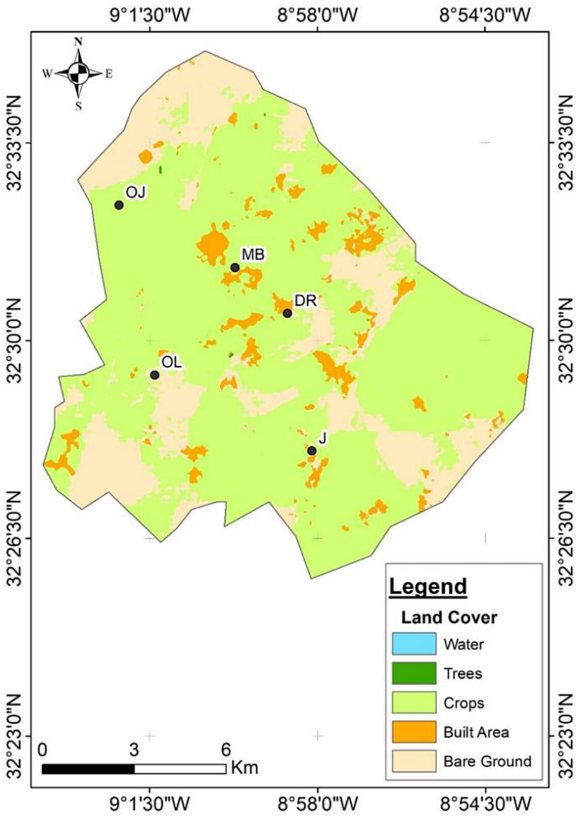

Figure 20. Land cover map in Moul El Bergui

parameter itself. After reclassifying all parameters using the Reclassify tool, the weighted sum tool in ArcGIS was used to assign weights to the different parameters, sum the maps, and generate the landslide susceptibility map. This resulting raster map, to which we added the location of certain cities in the region for ease of location, shows values ranging from 1.13 to 3.83. For ease reading and interpretation, these values were grouped by natural breaks method to five classes: very low (1.13–1.67), low (1.67–2.21), medium (2.21–2.75), High (2.75–3.29), and very high (3.29–3.83) as illustrated in Figure 22.

Susceptibility map has been classified in five categories, corresponding to values ranging from 1.13 to 3.83. The analysis shows that most of the territory studied falls into the Moderate and High categories, which together represent approximately 50.89% of the total area, indicating that more than half of the zone presents a moderate to high risk. These findings are also supported by geophysical prospections conducted in this area, which indicate that it is highly prone to karst cavities and collapses. The areas classified as Very High, covering 17.53% of the territory, probably correspond to the most sensitive areas, such as steep slopes, fractured or highly unstable rocky areas. Lower classes represent approximately 31.58% of the surface area, indicating areas that are relatively unexposed to landslides (Fig. 23).

Validation of the final map

Assessing the reliability of a prediction model is a crucial step in susceptibility mapping process (Deng et al., 2017). In this study, the resulting susceptibility map was evaluated using receiver operating characteristic curve and area under the curve metric (Vakhshoori et al., 2018). This approach quantifies agreement level between observed collapse locations used for validation and the predicted susceptibility results. A model is considered to have satisfactory predictive performance when the AUC value exceeds the reference threshold of 50% (Ali et al., 2025).

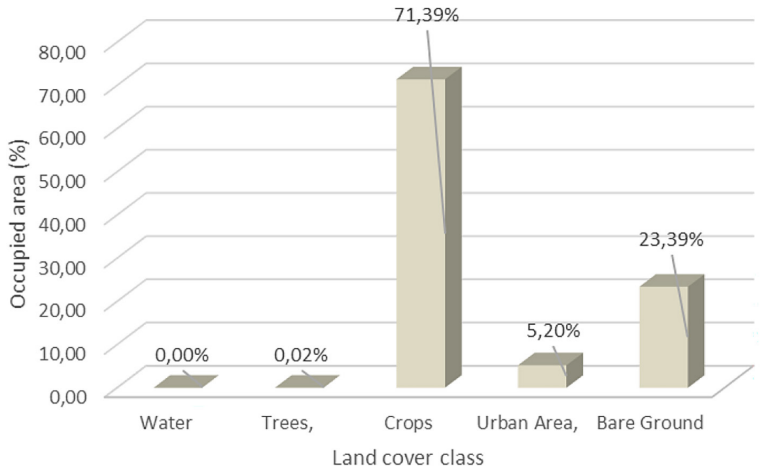

Figure 21. Bar chart of the area occupied by land cover class

Table 5. Judgment matrix

	P	Li	Sl	El	LC	NDVI	As	HND	FD
P	1	2	2	3	3	2	3	2	3
Li	0.50	1.0	2.0	2.0	3.0	3.0	3.0	5.0	2.0
Sl	0.50	0.50	1.0	2.0	3.0	3.0	3.0	3.0	2.0
El	0.33	0.50	0.50	1.0	3.0	3.0	3.0	3.0	3.0
LC	0.33	0.33	0.33	0.33	1.0	2.0	2.0	3.0	3.0
NDVI	0.50	0.33	0.33	0.33	0.50	1.0	2.0	3.0	3.0
As	0.33	0.33	0.33	0.33	0.50	0.50	1.0	3.0	3.0
HND	0.50	0.20	0.33	0.33	0.33	0.33	0.33	1.0	2.0
FD	0.33	0.50	0.50	0.33	0.33	0.33	0.33	0.50	1.0

Note: P – precipitation, Li – lithology, Sl – slope, El – elevation, LC – land cover, As – aspect, HND – hydrographic network density, FD – fracture density.

Table 6. Weighted judgment matrix with priority vector calculation

	P	Li	Sl	El	LC	NDVI	As	HND	FD	Priority vector
P	0.23	0.35	0.27	0.31	0.20	0.13	0.17	0.09	0.14	0.21
Li	0.12	0.18	0.27	0.21	0.20	0.20	0.17	0.21	0.09	0.18
Pt	0.12	0.09	0.14	0.21	0.20	0.20	0.17	0.13	0.09	0.15
Al	0.08	0.09	0.07	0.10	0.20	0.20	0.17	0.13	0.14	0.13
LC	0.08	0.06	0.05	0.03	0.07	0.13	0.11	0.13	0.14	0.09
NDVI	0.12	0.06	0.05	0.03	0.03	0.07	0.11	0.13	0.14	0.08
As	0.08	0.06	0.05	0.03	0.03	0.03	0.06	0.13	0.14	0.07
DRH	0.12	0.04	0.05	0.03	0.02	0.02	0.02	0.04	0.09	0.05
DF	0.08	0.09	0.07	0.03	0.02	0.02	0.02	0.02	0.05	0.04

AUC value obtained of 92.6% (Fig. 24), well above the reference threshold, indicating excellent model performance. This value confirms the reliability of the model, and its ability to correctly, predict areas prone to collapse.

The vulnerability map was established in the present article using the Geographic Information System method and analytic hierarchy process. This, taking into account the principal factors responsible for ground collapse, which

Table 7. Matrix consistency check

	P	Li	SI	EI	LC	NDVI	As	HND	FD	λi
P	0.21	0.37	0.30	0.39	0.26	0.16	0.20	0.09	0.13	10.08
Li	0.11	0.18	0.30	0.26	0.26	0.24	0.20	0.24	0.09	10.28
SL	0.11	0.09	0.15	0.26	0.26	0.24	0.20	0.14	0.09	10.40
EI	0.07	0.09	0.07	0.13	0.26	0.24	0.20	0.14	0.13	10.36
LC	0.07	0.06	0.05	0.04	0.09	0.16	0.13	0.14	0.13	10.03
NDVI	0.11	0.06	0.05	0.04	0.04	0.08	0.13	0.14	0.13	9.76
As	0.07	0.06	0.05	0.04	0.04	0.04	0.07	0.14	0.13	9.71
HND	0.11	0.04	0.05	0.04	0.03	0.03	0.02	0.05	0.09	9.45
FD	0.07	0.09	0.07	0.04	0.03	0.03	0.02	0.02	0.04	9.64
ACI						1.45	λmax			9.97
IC						0.12				
CR						8.37				

Table 8. Final weighting of judgment criteria

Symbol	Criteria	Weighting
P	Precipitation	21.0%
Li	Lithology	18.3%
SI	Slope	14.9%
EI	Elevation	13.0%
LC	Land cover	8.8%
NDVI	NDVI	8.1%
As	Aspect	6.7%
HND	Hydrographic network density	4.7%
FD	Fracture density	4.4%

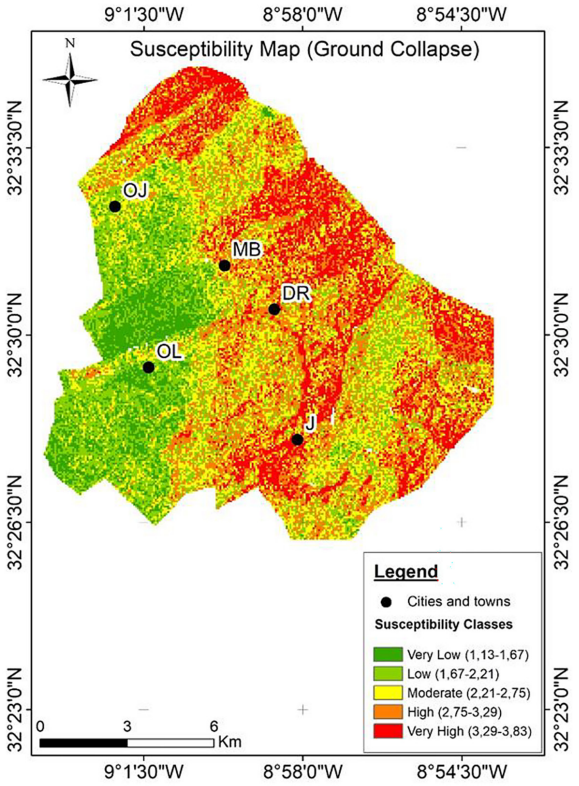

Figure 22. Final map of susceptibility to landslides in the municipality of Moul Bergui: MB – Moul Bergui, DR – Douar Rmel, OJ – Oulad Joudame, J – Jouadate, OL – Ouled Lahcen

are mainly topographical, geological, and hydrogeological. The precipitation factor represents the highest AHP weight of 0.21, followed by lithology (0.18). The weights for slope and elevation are 0.15 and 0.13, respectively. Afterwards, 0.09 and 0.08 for land cover and NDVI, respectively. Last, 0.07 for aspect, 0.05 for hydrographic density, and 0.04 for faults. These values show that groundwater flows are the main driver of karst collapses. In addition, slope plays an important role, as well as faults, in water infiltration. This later influences the rocks according to their lithology, particularly plio-quaternary sandstone and lower cretaceous limestone. Low NDVI and land cover can also increase water infiltration. The resulting map shows that moderate and high vulnerability classes dominate the study area. Validation of this map was performed using area under the curve, based on identified collapses and geophysical studies carried out in the area. The AUC percentage of 92.6% is very satisfactory and proves the reliability of the results. Thus, decision-makers can rely on these results to prevent the risk of karst collapse, thereby contributing to environmental protection and ecological sustainability.

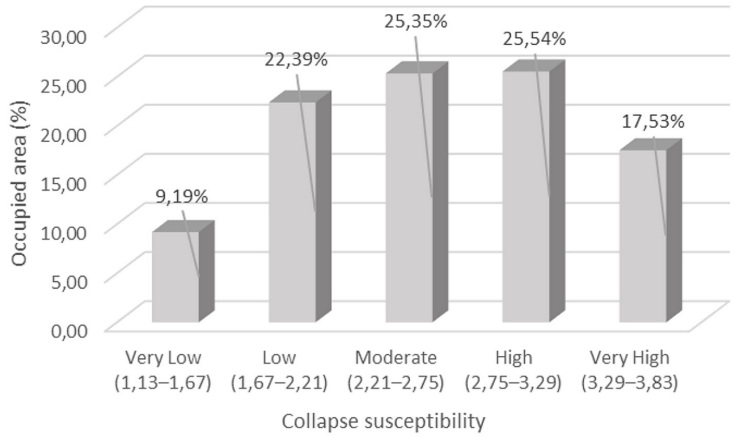

Figure 23. Bar chart of the area occupied by collapse susceptibility class

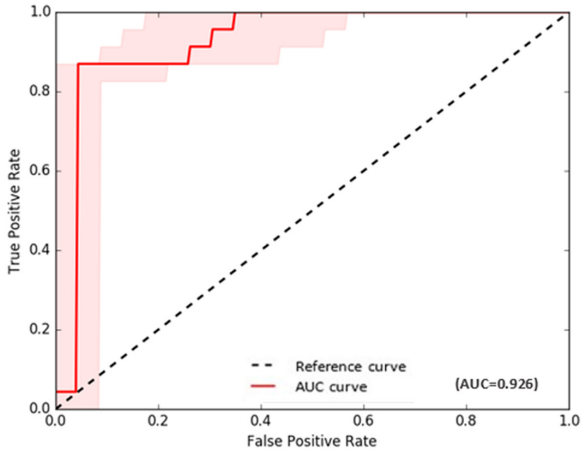

Figure 24. ROC (receiver operating characteristic) for assessing collapse susceptibility

CONCLUSIONS

This study successfully assessed the spatial susceptibility to ground collapse in the community of Moul El Bergui (Abda-Doukkala region, Morocco) and achieved its main objective of producing a reliable vulnerability map. The validation results confirm the robustness of the model, with a high predictive accuracy (AUC = 92.6%), indicating that the adopted approach is effective for identifying collapse-prone areas. The findings highlight that hydrogeological factors, particularly groundwater flow and precipitation, represent the main drivers of ground collapse, while lithology, slope, and faults also contribute significantly to water infiltration and subsurface instability. The predominance of moderate to high vulnerability classes reflects the sensitivity of the local geological formations, especially karstic and sedimentary units, to collapse phenomena. From a scientific standpoint, this research provides a spatial assessment of collapse susceptibility in a poorly studied Moroccan context, thereby filling an important regional gap in karst hazard analysis. Beyond its scientific contribution, the generated vulnerability map constitutes a practical decision-support tool for land-use planning, risk prevention, and sustainable territorial management.

REFERENCES

1. Ait El Haj, F., Ouadif, L., & Akhssas, A. (2023). Monitoring land use and land cover changes using remote sensing techniques and the precipitation-vegetation indexes in Morocco. *Ecological Engineering & Environmental Technology*, *24*. https://doi.org/10.12912/27197050/154937
2. Ali, A., Teku, D., Sisay, T., & Mihret, B. (2025). A combined analysis of frequency ratio and analytical hierarchy process for landslide susceptibility assessment in Tenta, South Wollo, Ethiopia. *Scientific Reports*, *15*(1), 17899. https://doi.org/10.1038/s41598-025-94611-z
3. Ayadi, O., Felfel, H., & Masmoudi, F. (2017). Analytic hierarchy process-based approach for selecting a Pareto-optimal solution of a multi-objective, multi-site supply-chain planning problem. *Engineering Optimization*, *49*(7), 1264–1280. https://doi.org/10.1080/0305215X.2016.1242913
4. Ben Brahim, F., Boughariou, E., Hajji, S., & Bouri, S. (2022). Assessment of groundwater quality with analytic hierarchy process, Boolean logic and clustering analysis using GIS platform in the Kebili's complex terminal groundwater, SW Tunisia. *Environmental Earth Sciences*, *81*(17), 419. https://doi.org/10.1007/s12665-022-10541-3
5. Boualla, O., Fadili, A., Najib, S., Mehdi, K., Makan,

A., & Zourarah, B. (2021). Assessment of collapse dolines occurrence using electrical resistivity tomography: Case study of Moul El Bergui area, Western Morocco. *Journal of Applied Geophysics*, *191*, 104366. https://doi.org/10.1016/j.jappgeo.2021.104366

6. Boualla, O., Mehdi, K., & Zourarah, B. (2016). Collapse dolines susceptibility mapping in Doukkala Abda (Western Morocco) by using GIS matrix method (GMM). *Modeling Earth Systems and Environment*, *2*(1), 9. https://doi.org/10.1007/s40808-015-0064-8
7. Bouchaqour, M., Ouadif, L., Bahi, L. Optimizing the exploitation of uus using ahp: a case study of rabat's city underground space, Morocco. (2023). *Journal of Southwest Jiaotong University*, *58*(4). https://doi.org/10.35741/issn.0258-2724.58.4.58
8. Bouroumine, Y., Bahi, L., Ouadif, L., Elhachmi, D., & Errouhi, A.A. (2020). Sitting MSW landfill combining GIS and analytic hierarchy process (AHP), Case study: Ajdir, Morocco. *International Journal of Advanced Research in Engineering and Technology (IJARET)*, *11*(5).
9. Deng, X., Li, L., & Tan, Y. (2017). Validation of spatial prediction models for landslide susceptibility mapping by considering structural similarity. *ISPRS International Journal of Geo-Information*, *6*(4), 103. https://doi.org/10.3390/ijgi6040103
10. Elhamdouni, D., Arioua, A., Karaoui, I., Ait Ouhamchich, K., Faouzi, E., & Aba, B. (2022). The multi-criteria analysis (AHP) method use for the environmental problems management: case of the household waste in Morocco. *Euro-Mediterranean Journal for Environmental Integration*, *7*(1), 13–20. https://doi.org/10.1007/s41207-022-00293-8
11. Erener, A, Mutlu, A., & Sebnem Düzgün, H. (2016). A comparative study for landslide susceptibility mapping using GIS-based multi-criteria decision analysis (MCDA), logistic regression (LR) and association rule mining (ARM). Eng Geol, *203*, 45–55
12. Guzzetti, F., Berti, M., Reichenbach, P., & Tofani, V. (2025). Landslide risk management in Italy: practices, advances, and future directions. Rendiconti Lincei. Scienze Fisiche e Naturali, 1–9. https://doi.org/10.1007/s12210-025-01382-w
13. Ibraheem, A.T., & Atia, N.S. (2016). Application of Analytical Hierarchy Process (AHP) for Multi-Storey Car Parks Location in a Small Area. Current Journal of Applied Science and Technology, *17*(5), 1–12. https://doi.org/10.9734/BJAST/2016/28596
14. Pourghasemi, H.R., Teimoori Yansari, Z., Panagos, P., & Pradhan, B. (2018). Analysis and evaluation of landslide susceptibility: a review on articles published during 2005–2016 (periods of 2005–2012 and 2013–2016). *Arabian Journal of Geosciences*, *11*(9), 193. https://doi.org/10.1007/s12517-018-3531-5
15. Rharouss, M., Benhaddou, K., Ouadif, L., Bouchaqour, M., & Menzhi, M. (2025). Contribution of geophysical methods for detecting underground cavities in the Abda-Doukkala region (Morocco). *Multidisciplinary Science Journal*, *7*(8), 2025368–2025368. https://doi.org/10.31893/multiscience.2025368
16. Wang Q., & Li W. (2017) A GIS-based comparative evaluation of analytical hierarchy process and frequency ratio models for landslide susceptibility mapping. Phys Geogr, 38(4), 318–337
17. Xie, Y.-H., Zhang, B.-H., Liu, Y.-X., Liu, B.-C., Zhang, C.-F., Lin, Y.-S., Xie, Y.-H., Zhang, B.-H., Liu, Y.-X., Liu, B.-C., Zhang, C.-F., & Lin, Y.-S., 2022. Evaluation of the Karst Collapse Susceptibility of Subgrade Based on the AHP Method of ArcGIS and Prevention Measures: A Case Study of the Quannan Expressway, Section K1379+300-K1471+920. Water, *14*. https://doi.org/10.3390/w14091432
18. Yalcin, A., Reis, S., Aydinoglu, A.C., & Yomralioglu, T (2011) A GIS-based comparative study of frequency ratio, analytical hierarchy process, bivariate statistics and logistics regression methods for landslide susceptibility mapping in Trabzon, NE Turkey. Catena, *85*(3), 274–287
19. Vakhshoori, V., & Zare, M. (2018). Is the ROC curve a reliable tool to compare the validity of landslide susceptibility maps? *Geomatics, Natural Hazards and Risk*, *9*(1), 249–266. https://doi.org/10.1080/19475705.2018.1424043
20. Wei, A., Li, D., Zhou, Y., Deng, Q., & Yan, L. (2021). A novel combination approach for karst collapse susceptibility assessment using the analytic hierarchy process, catastrophe, and entropy model. *Natural Hazards*, *105*(1), 405–430. https://doi.org/10.1007/s11069-020-04317-w
21. Zhou, L., Zhang, X., Shen, H., Zhang, D., & Bao, H., 2024. GIS analysis of urban ground collapse susceptibility: a case study of eastern Hangzhou, China. Front. Earth Sci. *11*. https://doi.org/10.3389/feart.2023.1338877
22. Zighmi, K., Zahri, F., Faqeih, K., Al Amri, A., Riheb, H., Alamri, S.M., & Alamery, E. (2025). AHP multi criteria analysis for landslide susceptibility mapping in the Tellian Atlas chain. *Scientific Reports*, *15*(1), 25747. https://doi.org/10.1038/s41598-025-10819-z